MOLECULAR AND CELLULAR BIOLOGY, Aug. 2003, p. 5269–5281 Vol. 23, No. 15
0270-7306/03/$08.00+0 DOI: 10.1128/MCB.23.15.5269–5281.2003

Human T-Lymphotropic Virus Type 1 Oncoprotein Tax Promotes Unscheduled Degradation of Pds1p/Securin and Clb2p/Cyclin B1 and Causes Chromosomal Instability

Baoying Liu,[1] Min-Hui Liang,[1] Yu-liang Kuo,[1] Wei Liao,[1] Imre Boros,[2] Tami Kleinberger,[3] Jan Blancato,[4] and Chou-Zen Giam[1]*

Department of Microbiology and Immunology, Uniformed Services University of the Health Sciences, Bethesda, Maryland 20814[1]; Institute of Biochemistry, Biological Research Center, Hungarian Academy of Sciences, H-6701 Szeged, Hungary[2]; Department of Molecular Microbiology, Faculty of Medicine, Technion-Israel Institute of Technology, Bat-Galim, Haifa 31096, Israel[3]; and Institute for Molecular and Human Genetics, Georgetown University, Washington, D.C. 20057[4]

Received 15 November 2002/Returned for modification 14 January 2003/Accepted 28 April 2003

Human T-lymphotropic virus type 1 (HTLV-1) is the causative agent of adult T-cell leukemia. The HTLV-1 transactivator, Tax, is implicated as the viral oncoprotein. Naïve cells expressing Tax for the first time develop severe cell cycle abnormalities that include increased DNA synthesis, mitotic arrest, appearance of convoluted nuclei with decondensed DNA, and formation of multinucleated cells. Here we report that Tax causes a drastic reduction in Pds1p/securin and Clb2p/cyclin B levels in yeast, rodent, and human cells and a loss of cell viability. With a temperature-sensitive mutant of the CDC23 subunit of the anaphase-promoting complex (APC), cdc23^{ts}; a temperature-sensitive mutant of cdc20; and a cdh1-null mutant, we show that the diminution of Pds1p and Clb2p brought on by Tax is mediated via the Cdc20p-associated anaphase-promoting complex, APC^{Cdc20p}. This loss of Pds1p/securin and Clb2p/cyclin B1 occurred before cellular entry into mitosis, caused a G_2/M cell cycle block, and was accompanied by severe chromosome aneuploidy in both *Saccharomyces cerevisiae* cells and human diploid fibroblasts. Our results support the notion that Tax aberrantly targets and activates APC^{Cdc20p}, leading to unscheduled degradation of Pds1p/securin and Clb2p/cyclin B1, a delay or failure in mitotic entry and progression, and faulty chromosome transmission. The chromosomal instability resulting from a Tax-induced deficiency in securin and cyclin B1 provides an explanation for the highly aneuploid nature of adult T-cell leukemia cells.

Human T-lymphotropic virus type 1 (HTLV-1) causes a malignancy of $CD4^+$ T lymphocytes called adult T-cell leukemia and a neurological disorder known as HTLV-1-associated myelopathy/tropical spastic paraparesis. Adult T-cell leukemia occurs in 2 to 6% of HTLV-1-infected individuals after a latency period of up to 20 to 40 years. The mechanism for progression from clinical latency to T-cell malignancy is not well understood but involves the unique viral transactivator-oncoprotein Tax, a regulatory protein critical for viral replication and T-cell transformation. Tax performs two major functions during the HTLV-1 life cycle: first, it mediates potent activation of viral transcription; second, it usurps regulatory mechanisms critical for cell growth and division to facilitate viral replication.

Although there is general agreement on the mechanism of Tax-mediated HTLV-1 long terminal repeat transactivation, the exact mechanism through which Tax promotes oncogenesis is not fully resolved. The effects that Tax exerts on cells are pleiotropic and include potent NF-κB activation (6, 16, 20, 45, 46), cell cycle perturbation (1, 8, 15, 24, 30–32, 38), and cell transformation (13, 29, 36, 46). More recently, Jin et al. reported that the interaction between Tax and the human spindle checkpoint protein HsMAD-1 causes a spindle checkpoint defect that results in DNA aneuploidy, microsatellite instability, and the formation of multinucleated giant cells (18, 21). In an earlier study, we showed that, in naïve mammalian cells, Tax expression causes multiple cell cycle aberrations that include activation of G_1/S entry, increased DNA synthesis, mitotic slowdown or arrest, and formation of multinucleated cells that apparently results from an uncoupling of DNA replication from cell division (25). Together, these results imply a role of Tax in perturbing critical mitotic functions.

Entry into mitosis requires both the accumulation of mitotic cyclins (cyclin B) and the activation of their associated kinases, Cdc2, Cdc28, and Cdk1 in the fission yeast *Schizosaccharomyces pombe*, the budding yeast *Saccharomyces cerevisiae*, and humans, respectively. The levels of mitotic cyclins are cell cycle regulated. They rise dramatically in late S phase, peak in G_2/M, and decline rapidly at the end of M phase (4, 9, 40). The abundance of mitotic cyclins is controlled by a multiprotein E3-ubiquitin ligase called the anaphase-promoting complex (APC) and its accessory factors: Cdc20p and Cdh1p. APC-mediated destruction of mitotic cyclins and other key regulators of mitosis is responsible for proper metaphase to anaphase transition and mitotic exit. Cdc20p-associated APC, APC^{Cdc20p}, initiates the ubiquitination and proteasome-mediated degradation of Clb2p/cyclin B1 and, most importantly, the ubiquitination and degradation of Pds1p (securin), a protein that sequesters the activator of sister chromatid separation, a

* Corresponding author. Mailing address: Department of Microbiology and Immunology, Uniformed Services University of the Health Sciences, 4301 Jones Bridge Rd., Bethesda, MD 20814. Phone: (301) 295-9624. Fax: (301) 295-1545. E-mail: giam@bob.usuf2.usuhs.mil.

TABLE 1. Strain list

Strain	Relevant genotype	Source
W303-1a	*MAT***a** *ade2-1 his3-11,15 leu2-3,112 trp1-1 ura3-1* ρ^+	Teresa Dunn
W303-PDS-HA	*MAT***a** *PDS1-HA*::*URA3 W303*	Orna Cohen-Fix
KY630	*CLB2-3×HA*::*URA3 W303*	Tami Kleinberger
AFS173	*MAT***a** *ade2-1 can1-100 his3-11,15 leu2-3,112 trp1-1 ura3-1 GFP-lacI*::*HIS3 lacO*::*LEU2*	Andrew W. Murray
785	*MAT***a** *cdc23-1 ura3 leu2 trp1 his3*	Angelika Amon
KH123	*MAT***a** *ura3-52 leu2-3,112 trp1 can1 ade2 his3-11,15 mad1Δ1*::*HIS3*	Tami Kleinberger
W321	*MAT***a** *ura3-1 leu2-3,112 trp1-1 ade2-1 his3-11,15 hct1Δ1*::*LEU2*	Tami Kleinberger
460	*MAT***a** *cdc20-1 ura3 leu2 trp1 his3*	Angelika Amon
785-PDS-HA	*MAT***a** *cdc23-1 ura3 leu2 trp1 his3 PDS1-HA*::*URA3*	This work
KH123-PDS-HA	*MAT***a** *ura3-52 leu2-3,112 trp1 can1 ade2 his3-11,15 mad1Δ1*::*HIS3 PDS1-HA*::*URA3*	This work
460-PDS-HA	*MAT***a** *cdc20-1 ura3 leu2 trp1 his3 PDS1-HA*::*URA3*	This work
W321-PDS-HA	*MAT***a** *ura3-1, leu2-3,112 trp1-1 ade2-1 his3-11,15 hct1Δ1*::*LEU2 PDS1-HA*::*URA3*	This work

protease called Esp1 (separin or separase). The destruction of Pds1p releases Esp1 (separase) to degrade Mcd1p/Scc1p, a component of the cohesin complex that is important for sister chromatid cohesion (7, 41). Proper control of Pds1p/securin degradation ensures normal metaphase to anaphase transition and faithful chromosomal transmission during mitosis. The importance of Pds1p/securin in chromosomal stability is best demonstrated by recent results showing that its loss results in abnormal anaphase and DNA aneuploidy (19). The APC^{Cdh1p} complex completes the degradation of cyclin B late in M phase and at the beginning of G_1 to ensure proper mitotic exit (47).

In this paper, we provide evidence that Tax perturbs mitotic entry and progression in *S. cerevisiae*, rodent, and human cells. As in mammalian cells, Tax expression in *S. cerevisiae* resulted in a G_2/M slowdown or arrest and a loss of cell viability. The mitotic defects caused by Tax are associated with a premature and drastic reduction in Pds1p and Clb2p levels mediated by APC^{Cdc20p}. In keeping with the critical roles of Pds1p/securin and Clb2p/cyclin B1 in mitosis, the aberrant diminution in both proteins as caused by Tax is accompanied by DNA aneuploidy in both *S. cerevisiae* and human cells. Our results support the idea that Tax promotes aberrant activation of APC^{Cdc20p} to block mitotic entry and progression. Coupled with its ability to activate G_1/S entry (25, 31, 32, 38), Tax apparently maintains cells in a metabolically active state that is favorable for viral replication. The mitotic defects induced by Tax, however, result in chromosomal instability that leads to severe DNA aneuploidy. These results provide a molecular explanation for the frequent chromosomal abnormalities in HTLV-1-infected T cells and the highly aneuploid nature of adult T-cell leukemia cells (10, 22, 26, 37).

MATERIALS AND METHODS

Cell culture. (i) Yeast strains, media, and growth conditions. Yeast cells were grown in YPAD (1% yeast extract, 2% Bacto-peptone, 2% glucose, and 0.01% adenine), YPGal (1% yeast extract, 2% Bacto-peptone, and 2% galactose), or synthetic complete (SC) medium with appropriate nutrient supplements. To induce Tax expression, cells were grown in SC medium with 2% raffinose overnight. They were then diluted to an A_{600} of 0.3 and allowed to grow for another 4 h, followed by the addition of galactose to 2%. Alternatively, cells were grown in 2% glucose to mid-log phase, washed once, and resuspended in SC medium containing 2% galactose. All yeast strains used are derived from W303, and a strain list is provided in Table 1.

(ii) Mammalian cell culture and media. PA18G-BHK-21 and HeLa cells were routinely cultured in Dulbecco's modified Eagle's medium (DMEM) supplemented with 10% fetal bovine serum (FBS), penicillin and streptomycin (100 U/ml each), and 2 mM L-glutamine. Human diploid fibroblast WI-38 cells were maintained in minimal essential medium (MEM) with the same supplements.

Plasmid construction. Centromere (CEN)-based expression plasmids for wild-type Tax, Gal10-Tax, were derived by inserting a 500-bp *Xho*I-*Nco*I fragment containing the galactose-inducible *GAL10* transcriptional regulatory region and a 1-kb *Nco*I-*Hin*dIII fragment carrying the *tax* cDNA into the *Xho*I and *Hin*dIII sites of plasmids pRS315 and pRS316 containing *LEU2* and *URA3* selection markers, respectively. The *Xho*I-*Sac*I fragment containing Gal10-Tax was taken from pRS316 and inserted into pRS314 to produce a similar CEN plasmid with a *TRP1* marker. The *tax*-null mutant Gal10-ΔTax was generated by filling in the *Nco*I site of Gal10-Tax to disrupt the *tax* reading frame.

***S. cerevisiae* cell cycle synchronization.** *S. cerevisiae* cells were first grown exponentially at 30°C to an A_{600} of 1 to 1.5 and then diluted to an A_{600} of 0.3 with addition of hydroxyurea (Fluka) to a final concentration of 0.2 M. After growth for another 3 h, the S-phase-arrested cells were centrifuged and washed with fresh medium. When appropriate, cells were treated with nocodazole (Fluka) for 4 to 5 h at a final concentration of 12 μg/ml.

***S. cerevisiae* immunoblot analysis, immunoprecipitation, and H1 kinase assay.** For immunoblots, yeast cells were harvested by centrifugation at 8,000 rpm in a microcentrifuge for 2 min. After removal of the supernatants by aspiration, cell pellets were frozen on dry ice. Typically, the cell pellet from 1.0 A_{600} of yeast cells was resuspended in 50 μl of distilled water by vortexing. An equal volume of 2× cracking buffer (0.1 M Tris-HCl, 20% glycerol, 4% sodium dodecyl sulfate, 2% β-mercaptoethanol, and 0.001% bromophenol blue) was then added. The cell suspension was boiled at 100°C for 5 min and frozen on dry ice again. After two additional freeze-boil cycles, unbroken cells and cell debris were pelleted by brief centrifugation in the microcentrifuge. The cell lysates were then analyzed by sodium dodecyl sulfate-polyacrylamide gel electrophoresis (SDS-PAGE) on a 12% gel (10 μl/lane) and by immunoblotting.

For immunoprecipitations, cell lysates were prepared by bead-beating yeast cells for 4 min at 4°C in 200 μl of lysis buffer (250 mM NaCl, 50 mM Tris-HCl [pH 7.4], 5 mM EDTA, 0.5% Nonidet P-40, 0.1% Triton X-100, 50 mM NaF, 100 mM sodium vanadate, 100 nM okadaic acid, and complete protease inhibitor cocktail). The extracts were spun to separate beads and cell debris from the clear lysates. The lysate was incubated with 3 μg of antihemagglutinin (anti-HA) antibody (Santa Cruz Biotechnology) at 4°C overnight. Protein G beads (Gibco-BRL) were then added for 90 min at 4°C to precipitate the immune complex.

For the H1 kinase assay, protein G beads were washed three times with 0.8 ml of lysis buffer and then suspended in 20 μl of kinase assay cocktail (20 mM morpholinepropanesulfonic acid [MOPS, pH 7.2], 25 mM β-glycerol phosphate, 5 mM EGTA, 1 mM sodium orthovanadate, 1 mM dithiothreitol). Ten microliters of HA-Clb2p immunoprecipitates were incubated with 10 μl of substrate cocktail (20 mM MOPS [pH 7.2], 25 mM β-glycerol phosphate, 5 mM EGTA, 1 mM sodium orthovanadate, 1 mM dithiothreitol) containing 2 mg of histone H1 (Upstate Biotechnology) per ml and 50 μCi of [γ-^{32}P]ATP (3,000 Ci/mmol) in 5 μl for 20 min. The reaction was stopped by the addition of 2× SDS-PAGE sample buffer, boiled for 5 min, resolved by SDS–12% PAGE. The phosphorylated histone H1 was then visualized by autoradiography.

***S. cerevisiae* flow cytometry and cell viability measurements.** One-milliliter culture samples were taken at the indicated times and collected by centrifugation in a microcentrifuge. Cells were resuspended and fixed in 500 μl of a buffer containing 3.7% formaldehyde in phosphate-buffered saline for microscopy. For flow cytometry, 10^7 cells were collected by brief centrifugation in a 1.5-ml Eppendorf tube. Ice-cold 70% ethanol (1 ml) was then added to the tube with

vortexing. Approximately 0.3 ml of the cell suspension was added to 3 ml of a solution containing 50 mM sodium citrate in a 5-ml Falcon tube. After mixing, cells were spun at 2,000 rpm for 5 min. The supernatant was discarded, and the cell pellet was resuspended in 0.5 ml of sodium citrate buffer containing 0.1 mg of RNase A per ml and incubated at 37°C for 2 h. Thereafter, 0.5 ml of sodium citrate buffer containing 8 μg of propidium iodide per ml was added to stain the DNA.

The cellular DNA content was determined by fluorescence-activated cell sorting (FACS) (Epics XL-MCL flow cytometer; Beckman-Coulter). Cells were either sorted by FACS immediately or stored overnight at 4°C in the dark and processed the next day. Cell viability was measured by first determining cell count with a hemacytometer. Approximately 500 cells were then plated on a YPD agar plate in triplicate and incubated at 30°C. Colonies were counted after 2 to 3 days.

Chromosome staining with GFP-LacI. AFS173, a W303-1a-derived strain (kindly provided by A. Murray) that contains 256 tandem copies of the *lac* operator (*lacO*) integrated at the *LEU2* locus on chromosome 3 and expresses a green fluorescence protein-Lac repressor (GFP-LacI) fusion protein under *HIS3* promoter control (27), was transformed with pGal10-Tax (wild-type Tax) or pGal10-ΔTax (ΔTax). AFS173/Gal10-Tax and AFS173/Gal10-ΔTax were grown to mid-log phase in SC medium containing 2% raffinose and then diluted to an A_{600} of 0.3 in the same medium supplemented with 2% galactose to induce Tax expression. After induction for 4 h, cells were transferred to SC medium without histidine but with 10 mM aminotriazole for 30 min to induce GFP-LacI expression. Cells were subsequently transferred to SC medium with 2% raffinose and 2% galactose and induced for Tax expression overnight or not. The next day, cells were washed, sonicated, and observed under the microscope to score GFP-stained chromosomes.

Production of recombinant adenovirus vectors. HEK 293 cells were grown to confluence (≈1.5×10^7 cells per T25 flask) in DMEM with 10% FBS and infected with the recombinant adenoviruses adeno-Tax and adeno-tTA (generous gifts from M. Yoshida and D. Morgan, respectively) in 2 ml of serum-free DMEM at a multiplicity of infection of 10. Cells were infected for 45 min with rocking every 5 to 10 min. Thereafter, 20 ml of DMEM supplemented with 2% FBS was added. Virus-infected cells were grown at 37°C for 3 to 4 days until approximately 70% of the cells detached from the plates, then harvested by centrifugation at $3,000 \times g$ for 5 min, and resuspended in phosphate-buffered saline with 10% glycerol. The cell suspension was then subjected to three freezing and thawing cycles over a dry ice-ethanol bath and a 37°C waterbath, with gentle vortex after each thawing. Cell debris was removed by centrifugation at $3,000 \times g$ for 10 min, and the virus solution was divided into aliquots and stored frozen at −70°C.

To determine the titer of the recombinant adenovirus vector, low-passage-number 293 cells were plated at 10^6 cells per well in a six-well plate 24 h before infection. The culture medium was then removed and replaced with fresh serum-free DMEM containing serially diluted viruses. Cells were infected for 1 h at 37°C with rocking every 15 min. The culture medium was removed, and each well of the plate was evenly overlaid with 2 ml of Opti-MEM containing 5% FBS and 0.5% low-melting-point agarose. The agarose overlay was prepared by mixing equal volumes of 1% low-melting agarose at 42°C with 10% FBS in Opti-MEM supplemented with L-glutamine and antibiotics at 37°C. Plaques usually appear in 7 to 10 days. To visualize plaque formation, 1 ml of a staining solution containing neutral red (0.03%; Quality Biologicals Inc., Gaithersburg, Md.) was added to each well for 2 h at 37°C. After removal of excess staining solution, the plates were put in the incubator overnight for the plaques to clear.

Synchronization of HeLa cells by double thymidine block and infection with recombinant adenovirus vectors. Two million HeLa cells were grown in 6 ml of DMEM containing10% FBS and 2.5 mM thymidine for 16 h. After an 8-h break in fresh serum-containing thymidine-free medium, cells were again grown in thymidine-containing medium for 16 h and released from the G_1/S block in DMEM containing 10% FBS. Eight hours into the second thymidine treatment, cells were infected at a multiplicity of infection of 10 with the adenovirus vectors adeno-Tax and adeno-tTA. After release from the G_1/S arrest, the cells were harvested at different times for flow cytometry (25) and Western blotting. Western blots were performed with Tax mouse hybridoma antibody (4C5) and rabbit polyclonal antibodies against cyclin B1 (Santa Cruz), actin (Santa Cruz), and human securin (kindly provided by H. Zou [48]).

Retroviral transduction, immunoprecipitation, and histone H1 kinase assay. The retroviral vectors pBabe-puro and pBabe-tax were produced as reported previously (25). From 50,000 to 100,000 PA18G-BHK-21 cells in a T-25 flask were infected with a high-titered stock of pBabe-puro or pBabe-tax at a multiplicity of infection of 10 and grown for 36 h. The cells were then harvested and divided into two portions for Western blot analysis and the H1 histone kinase assay. Western blot analysis was performed as described before (25). Antibodies against cyclin B1, cyclin D3, cyclin E, IκB-α, and actin were from Santa Cruz.

Histone H1 kinase assays were carried out as described above except that Cdk1 immunoprecipitated from lysates of pBabe-puro- or pBabe-tax-transduced PA18G-BHK-21 cells was used. Cell lysates were precleared by incubation with a 50% slurry of protein G-agarose (Life Technologies, Inc.) and 2 μg of normal rabbit antiserum for 30 min at 4°C. Immunoprecipitation was then carried out as described previously with 2 μg of a Cdk1 polyclonal antibody (Santa Cruz) and 200 μg of lysates from puromycin-selected PA18G-BHK-21 cells transduced with pBabe-puro or pBabe-tax. The immunoprecipitate was resuspended in 20 μl of H1 kinase reaction buffer, and the kinase reaction was carried out as detailed above.

Metaphase chromosome spread and chromosome analysis. Human diploid fibroblast WI-38 cells were infected with a high-titered stock of pBabe-puro or pBabe-tax retroviral vector at a multiplicity of infection of 10. Seventy-two hours postinfection, cells were fixed in colcemid (0.02 μg/ml) at 37°C for 30 min, stained with Giemsa (Life Technologies, Inc.) according to standard procedures, and examined by light microscopy.

RESULTS

Tax induces growth arrest and cell death in *S. cerevisiae*. During a LexA-based yeast two-hybrid screen, we noticed that *S. cerevisiae* cells harboring a LexA-Tax fusion grew significantly more slowly than the vector control. For this reason, we investigated the effect of direct expression of Tax on *S. cerevisiae* by constructing a galactose-inducible expression cassette for Tax, Gal10-Tax, and placing it in three centromere-containing, low-copy-number CEN plasmids with *URA3*, *LEU2*, and *TRP1* markers. The Gal10-Tax/*URA3*, Gal10-Tax/*LEU2*, and Gal10-Tax/*TRP1* constructs were used interchangeably to transform a standard haploid *S. cerevisiae* strain, W303-1a, and its derivatives. W303-1a/Gal10-Tax grew in raffinose-containing plates, on which Tax was not expressed (Fig. 1A, Raf), but failed to grow on galactose-containing plates, on which Tax expression was induced (Fig. 1B). By contrast, W303-1a/Gal10-ΔTax, which is W303-1a with a Tax-null control in which the ATG translational initiation site of the *tax* gene was disrupted by a frameshift mutation, grew equally well on both Raf- and Gal-containing plates (Fig. 1A, Raf+Gal). Consistent with this result, the growth of W303-1a/Gal10-Tax cells in liquid medium as measured by light absorbance (Fig. 1C) and cell number (Fig. 1D) became significantly reduced at 7 h and ceased at 23 h after galactose induction. Cell viability, determined by plating efficiency on YPAD plates, also declined as a function of Tax expression (Fig. 1E).

Tax-expressing *S. cerevisiae* cells become arrested at G_2/M. We have previously found that Tax activates cellular DNA synthesis but causes a mitotic arrest in naïve mammalian cells made to express Tax for the first time after retroviral transduction (25). To investigate whether Tax also causes a mitotic arrest in W303-1a cells, we grew W303-1a/Gal10-Tax cells in galactose medium and analyzed the time course of cell cycle progression by fluorescence-activated cell sorting (FACS). Consistent with the notion that Tax causes a mitotic arrest or slowdown, 6 h after galactose induction, W303-1a/Gal10-Tax cells but not the Tax-null control began to accumulate 2*N* DNA. By 7.5 and 9 h after induction, the majority of W303-1a/Gal10-Tax cells had accumulated at the G_2/M stage (Fig. 2A). Consistent with the G_2/M arrest, microscopic examination revealed an abundance of large-budded cells (74%) 7.5 h after galactose induction (Fig. 2B). Individual large cells with no buds were also readily seen, especially with longer galactose

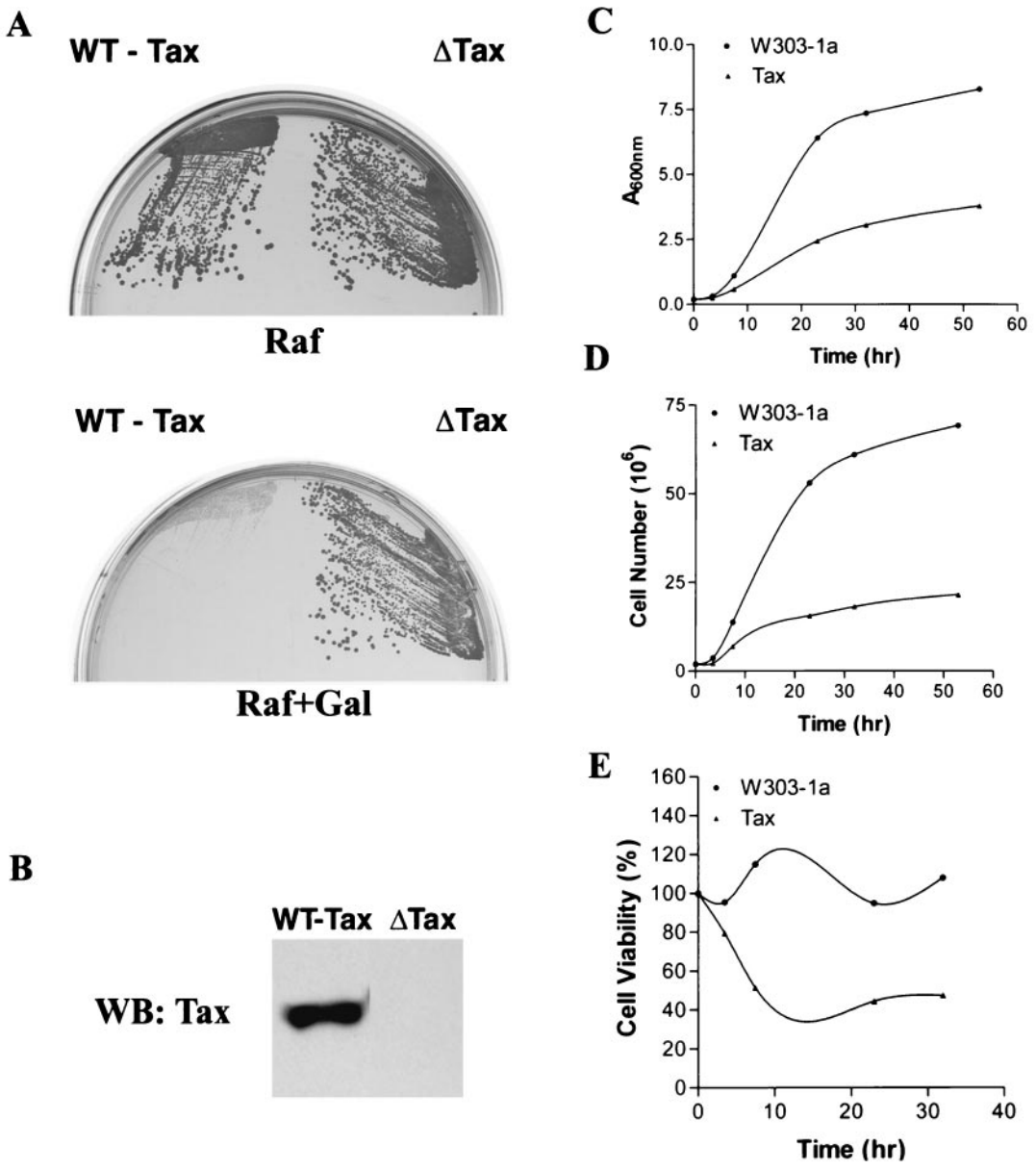

FIG. 1. Expression of HTLV-1 Tax causes growth arrest and loss of cell viability in *S. cerevisiae*. (A) W303-1a cells transformed with the Gal10-Tax (WT-Tax) or Gal10-ΔTax (ΔTax) plasmid were streaked on agar plates containing 2% raffinose (Raf) or 2% raffinose plus 2% galactose (Raf+Gal). Gal10-ΔTax is the same as Gal10-Tax except that the Tax reading frame was disrupted by filling in the *Nco*I site that overlaps the ATG translational start site. (B) Immunoblot (WB) analysis of HTLV-1 *tax* expression in *S. cerevisiae*. W303-1a/Gal10-Tax and W303-1a/Gal10-ΔTax were induced with galactose as described in Materials and Methods. Cell lysates were prepared, resolved on SDS–12% PAGE, transferred to a nitrocellulose membrane, and probed with a mouse monoclonal antibody against Tax. (C) W303-1a (solid circles) and W303-1a/Gal10-Tax (solid triangles) cells were grown in SC medium containing 2% raffinose and transferred to SC medium containing 2% raffinose with or without 2% galactose at time zero. Aliquots of cells were collected at different time points, and light absorbance at 600 nm was measured with a spectrophotometer. (D) The cell number in each aliquot was determined microscopically with a hemacytometer. (E) At different times after galactose induction, 500 cells each from W303-1a and W303-1a/Gal10-Tax were plated on YPAD plates for 2 days. Colony numbers were counted and normalized against the number of cells plated. Percent cell viability was plotted as a function of time after induction of Tax expression.

induction (not shown). Many of these large cells exhibited chromosomal segregation defects, as shown below.

Tax promotes Clb2p and Pds1p degradation in *S. cerevisiae*. Mammalian cells that express Tax for the first time develop severe cell cycle abnormalities that include increased DNA synthesis, mitotic arrest, appearance of convoluted nuclei and decondensed DNA, and uncoupling of DNA synthesis from cell division, which results in the formation of multinucleated cells (25). These phenomena can be explained by a reduction in the activity of the mitotic kinase cdk1-cyclin B1, which is critical for effecting the dramatic changes during mitosis that include (i) inhibition of DNA synthesis during G_2/M, (ii) chromosome condensation and nuclear membrane breakdown, (iii) formation of the mitotic spindle, (iv) sister chromatid separa-

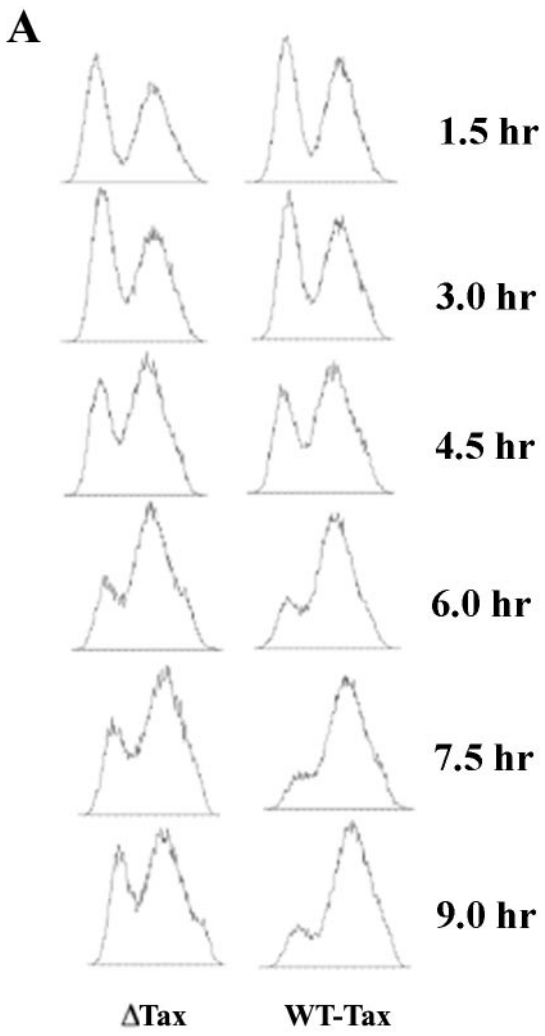

B

Cell Morphology

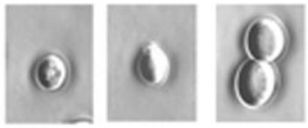

Time	Tax			
1.5 hr	–	52%	24%	24%
	+	58%	21%	21%
4.5 hr	–	14%	44%	42%
	+	9%	47%	44%
7.5 hr	–	28%	31%	41%
	+	7%	19%	74%

FIG. 2. Tax causes *S. cerevisiae* to undergo G_2/M cell cycle arrest. (A) W303-1a cells containing pGal10-Tax (WT-Tax) or pGal10-ΔTax (ΔTax)were grown in SC medium containing 2% raffinose overnight and then transferred to SC medium containing 2% raffinose and 2% galactose to induce Tax expression for the indicated durations. The cells were then fixed, stained with propidium iodide, and analyzed by flow cytometry. Note the decrease in the 1N population for Gal10-Tax cells at 6, 7.5, and 9 h after galactose induction. (B) At 1.5, 4.5, and 7.5 h postinduction, cells were observed under a light microscope and counted.

tion, and (v) possibly cytokinesis. For this reason, we examined whether Tax affects the Clb2p level in *S. cerevisiae*.

To this end, we introduced Gal10-Tax and Gla10-ΔTax into a W303-1a-derived yeast strain, KY630, in which the gene encoding Clb2 has been replaced with one encoding HA-tagged Clb2 (HA-Clb2p). After galactose induction at 30°C overnight, Tax-positive and Tax-negative cells were treated with nocodazole, and their Clb2p levels were determined. Nocodazole treatment activates the spindle checkpoint in normal cells, causing inactivation of APC^{cdc20p}, mitotic arrest, and accumulation of Pds1p and Clb2. Under these conditions, we found the Clb2p level of Tax-expressing cells to be greatly decreased compared to that of the Tax-negative control (Fig. 3A). The Cdc28-Clb2 activity in Tax-expressing cells was also significantly lower (Fig. 3A).

We next examined the effect of Tax on Clb2p levels during cell cycle progression. KY630/Gal10-Tax cells were grown to mid-log phase at 30°C and arrested at the G_1/S phase with hydroxyurea. The synchronized cells were divided into two parts and induced for Tax expression or not by the addition of 2% galactose or 2% glucose. At the same time, cells were released from cell cycle arrest, and their Clb2p levels were measured as a function of cell cycle progression. As shown in Fig. 3B, the Clb2p level of Tax-negative cells reached its peak at 1.5 h following the release from the G_1/S block and declined drastically at 2 h, indicating normal progression through mitosis, as confirmed additionally by FACS (Fig. 3B). By contrast, the Clb2p level of Tax-positive cells remained reduced at most if not all time points throughout the progression from S to G_2/M, with the greatest reduction seen at 1 h after release, and did not show significant cycling at the time point (2 h after release) when the Tax-negative cells had already exited mitosis (Fig. 3B). Consistent with the results in Fig. 2A, Tax-expressing cells became G_2/M arrested, as indicated by FACS (Fig. 3B, 1.5, 2, and 2.5 h postinduction).

The reduction in Clb2p level in Tax-expressing cells moti-

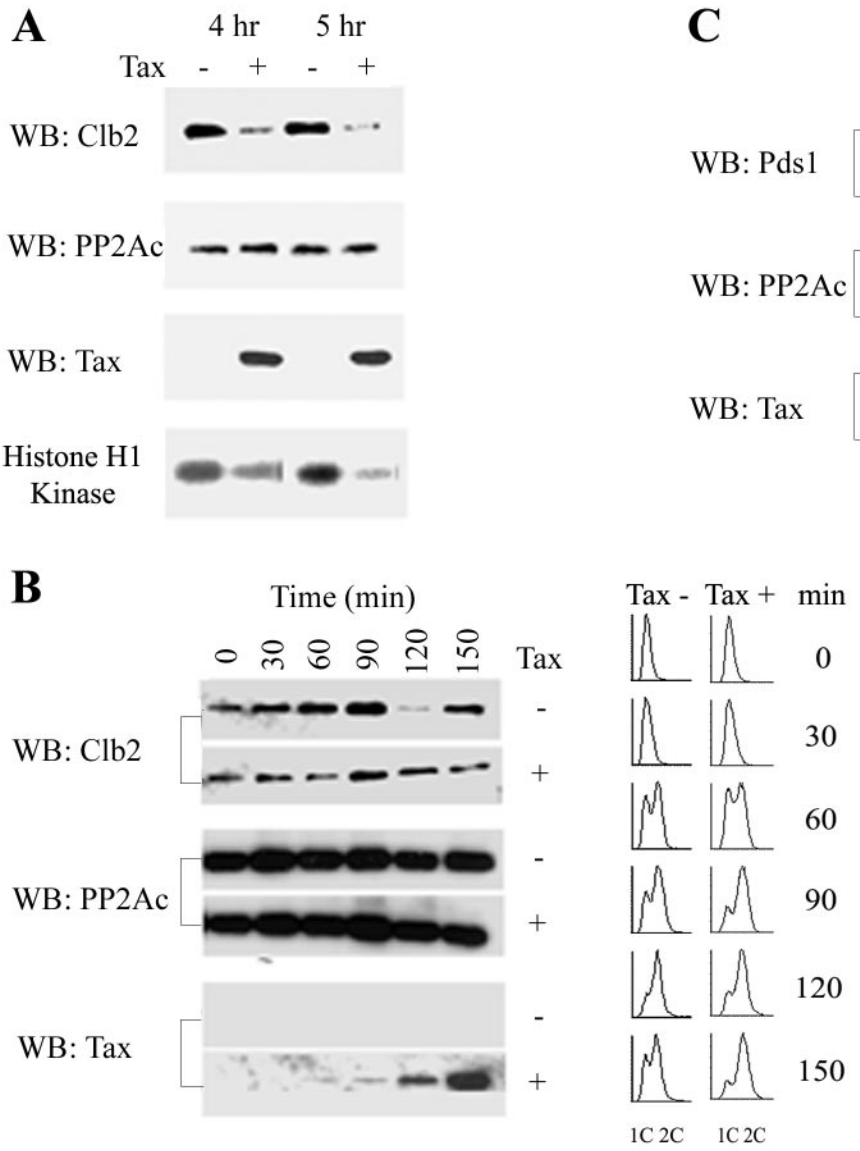

FIG. 3. Tax causes a drastic reduction in Clb2p and Pds1p levels in *S. cerevisiae*. (A) Tax causes a reduction in Clb2p level. KY630 cells carrying a gene encoding CLB2-3×HA integrated at the *CLB2* locus were transformed with either Gla10-ΔTax (lanes −) or Gal10-Tax (lanes +). After induction for 12 h in galactose-containing medium, cells were diluted to an A_{600} of 0.25 and treated with nocodazole (12 μg/ml) for 4 or 5 h. Immunoblots for Clb2 and Tax were carried out with anti-HA and 4C5 monoclonal antibodies, respectively. Immunoblotting (WB) for the catalytic subunit of protein phosphatase 2A (PP2Ac) was carried out as an internal protein control. Clb2-associated kinase activity (histone H1 kinase) was determined with histone H1 as a substrate (see Materials and Methods). (B) Tax promotes a reduction in Clb2p level prior to the onset of mitosis. KY630/Gal10-Tax cells were cultured in SC medium containing raffinose at 30°C overnight for 12 h, then diluted to 0.25 A_{600}, grown to mid-log phase, and treated with hydroxyurea (0.2 M) for 4 h to arrest cells at G_1/S. The synchronized cells were divided into two parts, induced for Tax expression (Tax +) or not (Tax −) by the addition of 2% galactose or 2% glucose, and simultaneously released from the cell cycle arrest. Cell lysates were prepared at the indicated times for Clb2, protein phosphatase 2A catalytic subunit, and Tax immunoblots as for panel A. Times after release and induction (0, 30, 60, 90, 120, and 150 min) are indicated. Flow cytometry was carried out as for Fig. 2A. (C) Tax causes a reduction in Pds1p level. W303-1a cells carrying a gene encoding Pds1-HA integrated at the *PDS1* locus were transformed with Gal10-Tax. Cells were grown at 30°C and synchronized with hydroxyurea as for panel B. Two hours into the hydroxyurea treatment, galactose or glucose was added to the culture to 2% to induce Tax expression or not for 2 h. Cells were then released from the cell cycle block in galactose-containing (rows +) or glucose-containing (row −) medium. Cell lysates were prepared and blotted for Pds1p-HA, protein phosphatase 2A catalytic subunit, and Tax as before. Times (0, 30, 60, 90, and 120 min) after release from G_1/S arrest are indicated.

vated us to examine whether the level of Pds1p, another key mitotic regulator that is regulated similarly to Clb2p, is also affected by Tax. To this end, we transformed a W303-1a derivative that encodes HA-tagged Pds1p with Gal10-Tax. Cells were then grown at 30°C and synchronized at the G_1/S boundary with hydroxyurea treatment. At 2 h after hydroxyurea treatment, Tax expression was induced (or not) by the addition of galactose (or glucose) for 2 h in the presence of hydroxyurea. This condition is slightly different from that in the experiment shown in Fig. 3B and allows accumulation of Tax to occur

before release of the cell cycle arrest (Fig. 3C, bottom panel, for Tax expression). Cells were then released from the G_1/S arrest and analyzed for Pds1p by immunoblotting. As indicated, the level of Pds1p in Tax-negative cells increased as a function of time after release from the G_1/S block and declined as cells progressed through mitosis (Fig. 3C, 90 min after release). By contrast, the Pds1p level of Tax-positive cells was significantly reduced at the time of release through the cell cycle progression and persisted at a reduced level beyond the point when the Tax-negative cells had exited mitosis, much like what was observed for Clb2p (Fig. 3B). These data indicate that the Tax-induced G_2/M arrest correlate with a decrease in Pds1p and Clb2p before cellular entry into mitosis, possibly via unscheduled degradation.

APC^{Cdc20p} mediates Tax-induced decreases in Pds1p and Clb2p levels. We next tested whether the effect of Tax on Pds1p and Clb2p involves APC. Cdc23p is a tetratricopeptide repeat protein that constitutes one of the subunits of APC E3 ubiquitin ligases. Ablation of Cdc23p inactivates APC. A W303-1a-derived yeast strain, 785-*cdc23^{ts}* (a generous gift of A. Amon), containing a temperature-sensitive *cdc23* mutation was transformed with the Gal10-Tax plasmid. For ease of detection, the *PDS1* gene in this strain was also replaced with *PDS1* encoding an HA tag (kindly provided by O. Cohen-Fix). *cdc23^{ts}*/Gal10-Tax cells grown to mid-log phase at 23°C were treated with hydroxyurea for 2 h and divided into four portions, each grown at 23°C or 37°C in hydroxyurea- and galactose- or glucose-containing medium for 2 h more (to maintain cell cycle arrest and induce Tax expression or not at the same time). The cells were then released from the G_1/S arrest in hydroxyurea-free but galactose- or glucose-containing medium for 1 h and blotted for Pds1p and Clb2p (Fig. 4A). A *CDC23* wild-type control was also carried out at 37°C to make certain that the activity of Tax is seen at that temperature.

As expected, at the permissive temperature of 23°C, Tax caused a reduction in Pds1p and Clb2p levels (Fig. 4A, left panel). Importantly, at the nonpermissive temperature of 37°C, inactivation of Cdc23p in *cdc23^{ts}*/Gal10-Tax cells significantly mitigated Tax-induced Pds1p and Clb2p degradation (Fig. 4A, middle panel). As anticipated from the results in Fig. 3, under the same conditions, the effect of Tax on the decrease in Pds1p and Clb2p remained unchanged in *CDC23* (wild-type) cells at 37°C (Fig. 4A, right panel, WT). Tax activity was seen at all time points preceding the time (2 h after release) when Tax-negative cells exited mitosis. The results at 1 h after the release from G_1/S block are shown.

Because APC^{Cdc20p} is responsible for the destruction of Pds1p and for initiating the degradation of Clb2p, we surmised that the effect of Tax on Pds1p and Clb2p is most likely mediated by APC^{Cdc20p}. This would be consistent with the data showing that Tax causes a reduction in Pds1p level (Fig. 3C) and that a reduced by detectable level of Clb2p persisted in the presence of Tax (Fig. 3B). To investigate whether APC^{Cdc20p} or APC^{Cdh1p} mediates the activity of Tax, we expressed Tax in a temperature-sensitive *CDC20* (*cdc20^{ts}*), a *mad1*-null, and a *cdh1*-null mutant with the same conditions as above. As shown in Fig. 4B, the effect of Tax on Pds1p and Clb2p could be seen in the *cdh1*-null mutant (Fig. 4B, *cdh1*Δ), in the *cdc20^{ts}* mutant at the permissive temperature (Fig. 4B, cdc20^{ts}, 23°C), and in the *mad1*-null mutant (Fig. 4B, mad1Δ), but not in the *cdc20^{ts}* mutant at the nonpermissive temperature (Fig. 4B, cdc20^{ts}, 37°C).

A closer examination of the results from the *cdh1*-null mutant further strengthened the notion that APC^{Cdc20p} is the target of Tax. The destruction of Cdc20p is mediated by APC^{Cdh1p} (33, 34, 35, 44). Because Pds1p degradation is mediated by APC^{Cdc20p}, if Tax activates APC^{Cdc20p}, then one might reasonably expect that the effect of Tax on Pds1p will be further exaggerated when Cdc20p degradation is prevented in a *cdh1*-null background. This was indeed the case. As shown in Fig. 4C, the level of Pds1p became drastically diminished when Tax expression was induced in the *cdh1*-null cells (Fig. 4C, compare Tax$^+$ and Tax$^-$ in *cdh1*Δ cells; also see Fig. 3C for a comparison with wild-type *CDH1*). In aggregate, these results support the notion that activation of APC^{Cdc20p} by Tax is responsible for the G_2/M arrest and the unscheduled degradation of Pds1p and Clb2p.

Tax promotes aberrant cyclin B1 degradation in mammalian cells. Prompted by earlier results showing that Tax causes a mitotic block in mammalian cells (25) and the data from *S. cerevisiae* described above, we examined the effect of Tax on cyclin B1 and securin in mammalian cells. We have previously generated a retroviral vector, pBabe-tax, with the murine leukemia virus-based retrovirus vector pBabe-puro (25). High-titered retroviral stocks pseudotyped with the vesicular stomatitis virus envelope glycoprotein were produced for pBabe-tax and pBabe-puro as previously described (25) and used to infect a baby hamster kidney (BHK) cell line, PA18G-BHK-21 cells, which harbor a reporter cassette comprising the *lacZ* gene under the control of the HTLV-1 long terminal repeat. The expression of LacZ in PA18G-BHK-21 is highly dependent on Tax and little β-galactosidase activity could be detected in its absence (25). This allows Tax expression to be readily scored.

To determine whether Tax affects cyclin B levels, PA18G-BHK-21 cells were starved for serum for 24 h and then infected with pBabe-puro or pBabe-tax (wild-type Tax) vector at a multiplicity of infection of 10. Infected cells were then grown in DMEM containing 10% fetal bovine serum for 36 h. Total cell lysates were prepared from each treatment and analyzed for the levels of cyclin B1, Tax, cyclin D3, cyclin E, IκB-α, and actin (as a control for protein loading). As predicted from the results with *S. cerevisiae*, the level of cyclin B1 (Fig. 5A) and the mitotic Cdk1/Cdc2 kinase activity (Fig. 5B) became significantly reduced in Tax-transduced cells. In agreement with the well-established paradigm that Tax potently activates IκB kinase to bring about constitutive phosphorylation and degradation of IκB-α, the level of IκB-α in Tax-transduced cells also decreased significantly (Fig. 5A). In contrast, both cyclin D and cyclin E levels became higher in Tax-expressing cells, consistent with activation of DNA synthesis by Tax, as reported previously (25, 31, 32, 38).

Tax promotes premature cyclin B1 and securin degradation in synchronized HeLa cells. We next synchronized HeLa cells at the G_1/S phase of the cell cycle by a double 16-h thymidine block. Eight hours into the second thymidine treatment, HeLa cells were infected with either a recombinant adenovirus vector that expressed Tax (adeno-Tax) or a control adenovirus vector that expressed the Tet activator (adeno-tTA), at a multiplicity of infection of 10. After release of the infected cells from the G_1/S block, their progression through the cell cycle was ana-

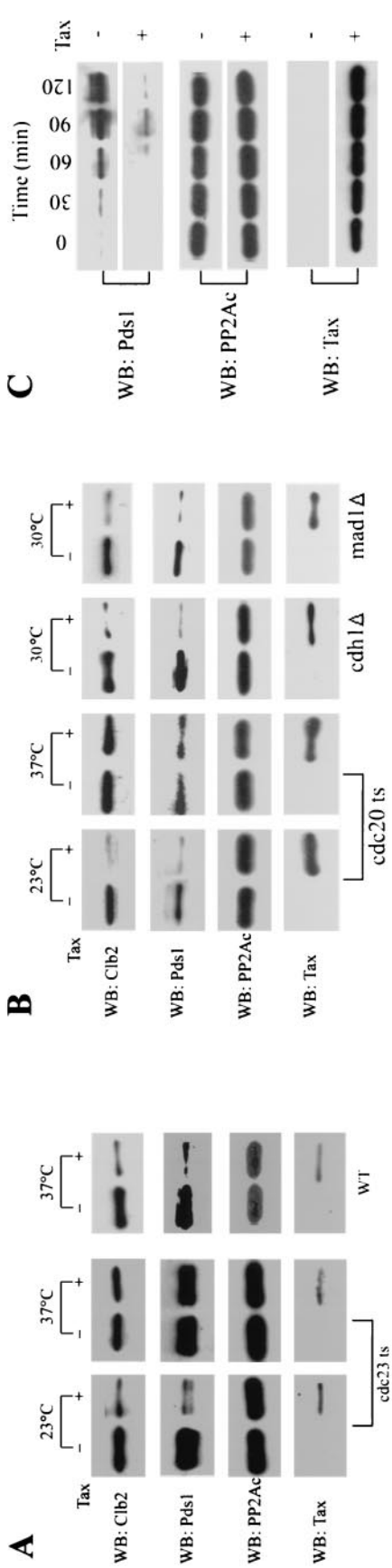

FIG. 4. APC^{Cdc20p} mediates Tax-induced Pds1p and Clb2p degradation. (A) The *PDS1* gene in the W303-1a-derived strain 785-$cdc23^{ts}$ was replaced with a gene encoding HA-Pds1. The resultant strain was further transformed with the Gal10-Tax plasmid. $Cdc23^{ts}$/Gal10-Tax cells grown to mid-log phase at 23°C were treated with hydroxyurea for 2 h and divided into four portions, each grown at 23°C or 37°C in hydroxyurea- and galactose- or glucose-containing (Tax + and Tax −, respectively) medium for 2 h more (to maintain cell cycle arrest and induce Tax expression or not at the same time). The cells were then released from the G_1/S arrest in medium without hydroxyurea but with galactose or glucose (to induce Tax expression or not) for 1 h and blotted for Pds1p and Clb2p (left and middle panels). W303-1a/Gal10-Tax grown at 37°C under the same conditions was included as a control (WT, right panel). Cell lysates were prepared at 1 h after release. Immunoblots (WB) for Clb2p, Pds1p-HA, protein phosphatase 2A catalytic subunit (PP2Ac), and Tax were carried out as before. Clb2p antibody was from Santa Cruz. (B) The *PDS1* genes in a $cdc20^{ts}$, a *mad1*-null (mad1Δ), and a *cdh1*-null (cdh1Δ) derivative of W303-1a were replaced with the gene encoding HA-Pds1 as above. The resultant strains were transformed with the Gal10-Tax plasmid. The conditions for cell cycle arrest, Tax induction, temperature shift, release from G_1/S block, and immunoblotting were as for panel A. The experiments for $cdc20^{ts}$ were carried out at 23°C and 37°C, and those for the *cdh1*-null and *mad1*-null mutants were done at 30°C. (C) The Tax phenotype is exaggerated in the *cdh1*-null background. Cell cycle arrest, Tax induction, release from G_1/S block, and immunoblotting were as for panel A. Times after release from G_1/S arrest (0, 30, 60, 90, and 120 min) are indicated.

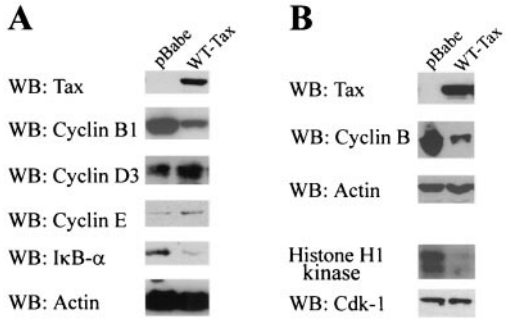

FIG. 5. Dramatic reduction in cyclin B1 level in Tax-expressing rodent cells. (A) BHK cells harboring the HTLV-1 long terminal repeat-*lacZ* reporter construct were starved for serum for 24 h and then infected with the pBabe-puro (pBabe) or pBabe-tax (WT-Tax) retrovirus vector at a multiplicity of infection of 10. The cells were then grown in DMEM containing 10% fetal bovine serum for 36 h. Total cell lysates were prepared from each treatment and analyzed for the levels of Tax, cyclin B1, cyclin D3, cyclin E, IκB-α, and actin (as a control for protein loading) by immunoblotting (WB) with the respective antibodies. (B) BHK cells were infected with the pBabe-puro (pBabe) or pBabe-tax (WT-Tax) retrovirus vector as for panel A. Cells were harvested and divided into two portions for Western blot (WB) analysis (Tax, cyclin B1, and actin) and the immunoprecipitation/H1 histone kinase assay. For Cdk1 assays, cell extracts were immunoprecipitated as described in Materials and Methods. One half of the Cdk1 immunoprecipitates was suspended in SDS-PAGE loading buffer, resolved by SDS–12% PAGE, and blotted with a rabbit polyclonal antibody against Cdk1 (WB: CDK1). The other half of the immunoprecipitates was assayed for Cdk1 kinase activity with histone H1 as a substrate as described in Materials and Methods. The phosphorylated histone H1 was visualized by autoradiography (histone H1 kinase).

lyzed by flow cytometry (Fig. 6A), and their levels of cyclin B1 and securin were measured at various times (Fig. 6B).

As expected, adeno-tTA-infected cells cycled normally. Their levels of cyclin B1 and securin rose before mitosis (6 to 8 h after release) and fell drastically after mitosis (12 h after release; Fig. 6B, adeno-Tax − lanes). In contrast, and in agreement with the data obtained from *S. cerevisiae* and BHK cells, adeno-Tax-infected cells became slowed down or arrested at G_2/M (Fig. 6A, compare adeno-tTA-infected and adeno-Tax-infected cells at 8 and 12 h after release), with their cyclin B1 and securin levels becoming significantly reduced soon after Tax expression and before the onset of mitosis (see the adeno-Tax + lanes at 0, 4, 5, and 6 h after release from G_1/S arrest). At 12 h after release from the G_1/S block, the majority of the adeno-tTA-infected cells had exited mitosis, while more than half of the adeno-Tax-infected cells remained arrested at G_2/M, as indicated by flow cytometry and cyclin B and securin immunoblots (Fig. 6).

Tax causes infidelity in chromosome segregation and DNA aneuploidy. As alluded to earlier, the surge in Clb2p/cyclin B levels and Cdc28-clb2 or Cdk1-cyclin B1 activity is crucial for the dramatic changes that occur during mitosis to ensure the faithful transmission of chromosomes into daughter cells. The orderly degradation of Pds1p/securin and Clb2p/cyclin B is critical for controlling sister chromatid separation and mitotic exit, respectively. The severe deficiency in both proteins prior to mitosis induced by Tax can therefore adversely impact faithful chromosome transmission. With this in mind, we examined the fidelity of chromosome segregation in Tax-expressing cells.

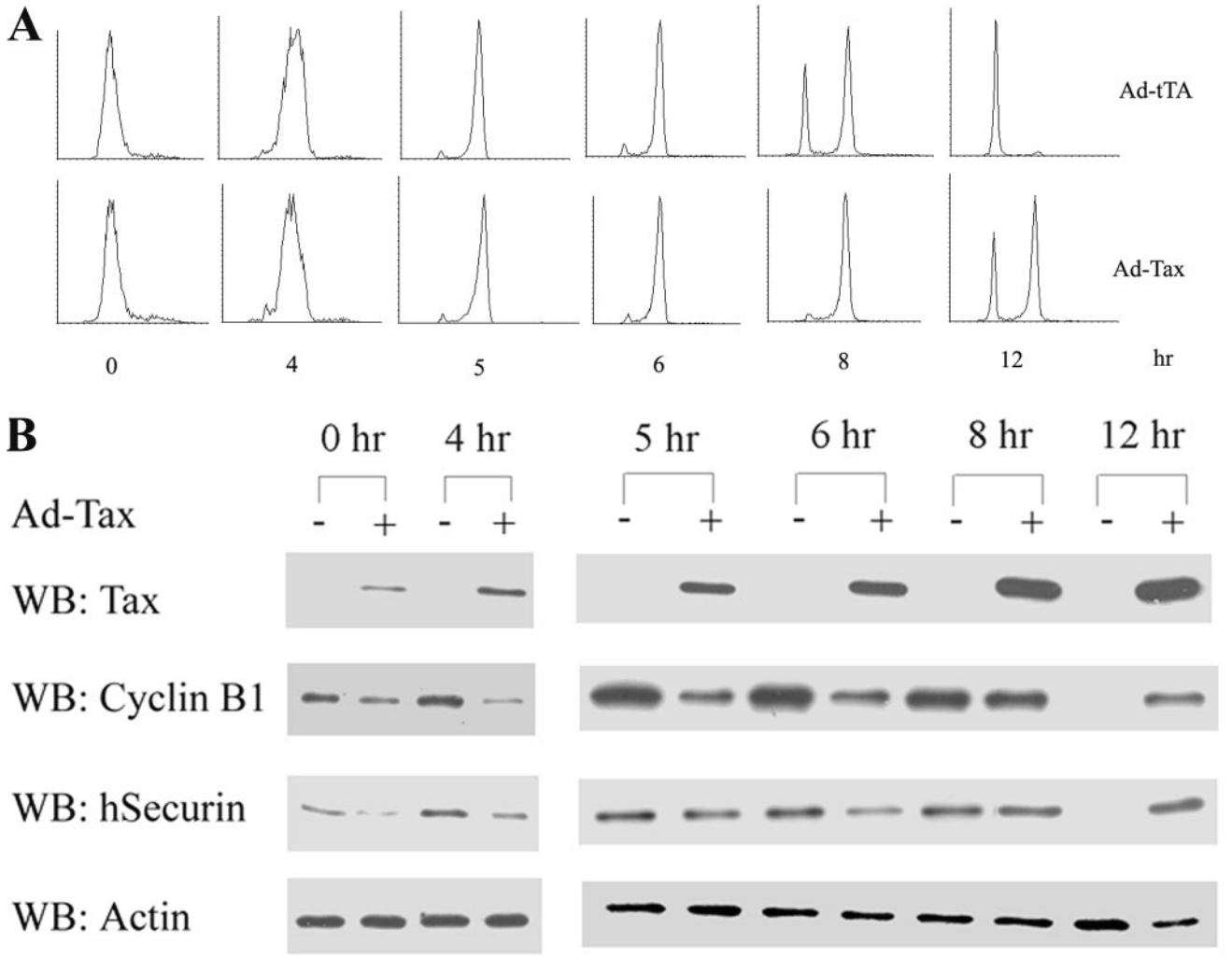

FIG. 6. Tax promotes premature degradation of securin and cyclin B1 in human cells. HeLa cells were synchronized by a double thymidine block and infected with a recombinant adenovirus vector that expresses Tax, adeno-Tax (Ad-Tax, lanes +) or a control adenovirus vector that expresses the Tet activator, adeno-tTA (Ad-tTA, lanes −) as described in Materials and Methods. Cells were released from the G_1/S arrest for the times indicated and (A) analyzed by FACS and (B) immunoblotted for Tax, cyclin B1, human securin (hSecurin), and actin.

To this end, we introduced the Gal10-Tax and Gal10-ΔTax plasmids into a W303-1a-derived strain whose chromosome III is marked by a tandem array of 256 copies of the *lac* operator site and a gene encoding a GFP-LacI fusion protein (kindly provided by Andrew Murray).

Induction of Tax expression by galactose overnight led to the production of single cells with two fluorescence signals at a high frequency (Fig. 7A, wild-type Tax). The fraction of Tax-expressing cells with multiple fluorescence signals was estimated to be approximately 30%. Single cells with three or four fluorescence signals were also readily detected (Fig. 7A, inset). Under the same growth condition, the majority of Tax-null cells (Gal10-ΔTax) showed a single fluorescence signal emanating from chromosome III (Fig. 7A, ΔTax). For reasons that are unclear at present, Tax-positive cells with chromosomal abnormalities appeared enlarged compared to the normal Tax-null cells. They appeared to have grown in an isotropic manner and failed to partition chromosomes properly.

To demonstrate that Tax causes infidelity in chromosome segregation in human cells, we infected human diploid fibroblast WI-38 cells with vesicular stomatitis virus glycoprotein-pseudotyped pBabe-puro or pBabe-tax at a multiplicity of infection of 10 for 72 h and analyzed 20 cells each for chromosome ploidy by metaphase chromosome spread. As shown in Table 2, the control pBabe-puro-infected WI-38 cells consisted of two populations (8 and 12 cells each) containing 43 and 46 chromosomes, respectively. The pBabe-tax-transduced WI-38 cells, by contrast, exhibited dramatic DNA aneuploidy, with chromosome numbers ranging from 44 to 134, with a modal number of 69 (Table 2). The metaphase chromosome spread of a Tax$^+$ WI-38 cell that showed severe aneuploidy (≈120 chromosomes) and that of a Tax-negative control are shown in Fig. 7B (denoted pBabe-tax and pBabe, respectively). Together, these results support the notion that the aberrant degradation of Pds1p/securin and cyclin B induced by Tax leads to a failure in proper chromosome segregation and mitosis.

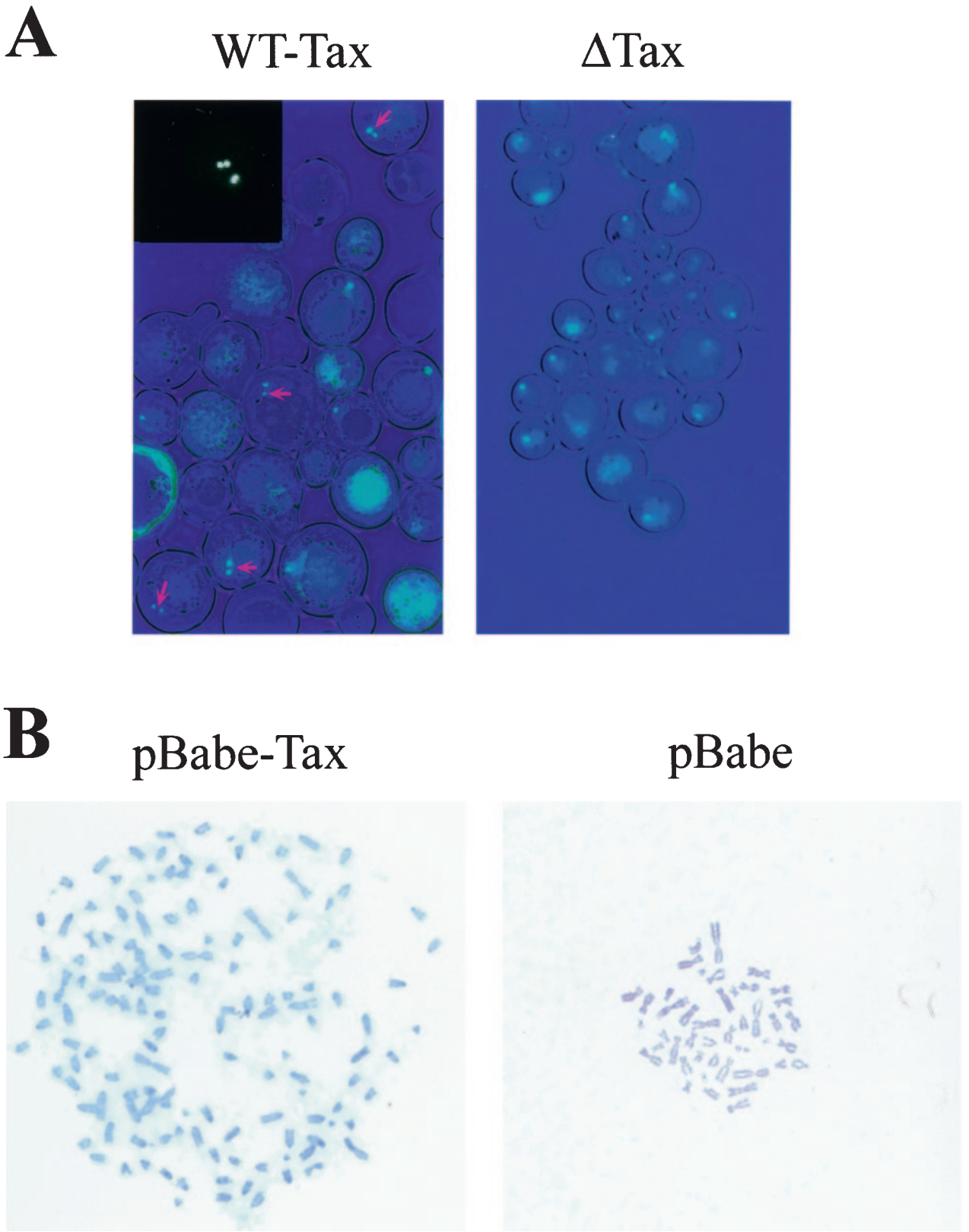

FIG. 7. Tax induces a chromosome segregation defect in *S. cerevisiae* and human cells. (A) AFS173 cells containing Gal 10-Tax or Gal10-ΔTax were induced for LacI-GFP and Tax or ΔTax expression as described in Materials and Methods. Fluorescence microscopy was carried out with an Olympus IX70 microscope. WT-Tax, Tax^+ cells containing two or more fluorescent spots are marked with arrows. Inset: a Tax^+ cell with at least three fluorescent spots. ΔTax, Tax-null cells with single fluorescence spots. (B) Metaphase chromosome spread of human diploid fibroblast WI-38 cells infected with a high-titered stock of the pBabe-tax or pBabe-puro (pBabe) retrovirus vector.

TABLE 2. Karyotypic abnormalities of Tax-expressing WI-38 diploid cells[a]

No. of chromosomes	No. of cells (n = 20)	
	pBabe-puro	pBabe-tax
43	8	0
44	0	1
46	12	0
65	0	1
66	0	2
67	0	1
68	0	4
69	0	4
70	0	4
72	0	2
134	0	1

[a] Babe-puro and pBabe-tax retrovirus vector-infected WI-38 cells were examined by metaphase chromosome spread. The chromosome numbers of 20 cells each were tabulated.

DISCUSSION

In this study, we have shown that expression of HTLV-1 *tax* in *S. cerevisiae* results in a block of the cell cycle at the G_2/M stage and loss of cell viability. We further demonstrate that the Tax-induced cell cycle defects correlated with a drastic reduction in Pds1p and Clb2p levels in *S. cerevisiae*. This diminution in Pds1p and Clb2p levels and the accompanying decrease in Cdk1/Cdc28 activity occur prior to cellular entry into mitosis and are APC^{Cdc20p}-mediated. A similarly drastic decline in cyclin B1 and securin was seen in Tax-expressing rodent and human cells. The mitotic aberrations elicited by Tax led to impaired chromosome segregation and severe DNA aneuploidy, among other cellular abnormalities.

A surge in cyclin B level and mitotic cyclin-dependent kinase activity is required to effect the striking cellular changes that occur during mitosis. Our results indicate that the premature degradation of Pds1p/securin and cyclin B caused by Tax delays or prevents proper mitotic entry and progression. Coupled with the ability of Tax to activate G_1/S entry and NF-κB, the mitotic block or slowdown brought on by Tax possibly keeps HTLV-1-infected cells in a metabolically active state to support viral replication. Because heightened Cdk1-cyclin B1 activity at the G_2/M boundary prevents new rounds of DNA synthesis after S phase and promotes chromosome condensation, nuclear membrane breakdown, spindle assembly, and other mitotic functions, we think that the dysregulated DNA replication, formation of multinucleated cells (with multiple nuclei in a chain or a cluster), and cytokinesis defect seen in Tax-expressing cells (25) may be largely due to the aberrant destruction of cyclin B and diminution of Cdk1-Cyclin B1 activity. This deficiency is further exacerbated by the premature degradation of Pds1p/securin, so that a severe abnormality in sister chromatid separation ensues.

It has recently been shown that the release of Esp1p/separase from Pds1p/securin inhibition is necessary but not sufficient for the former to become active (39). When the Clb2p/cyclin B1 level is high, separase is phosphorylated at serine residue 1126 and remains inactive in the absence of Pds1p/securin (28). Thus, both the degradation of Pds1p/securin and a reduction in Clb2p/cyclin B1 level are needed for Esp1p/separase to become active and sister chromatid separation to commence. The drastic fall in Pds1p/securin and Clb2p/cyclin B1 levels caused by Tax most likely leads to aberrant separase activation, the consequences of which, loss of sister chromatid cohesion and faulty chromosome transmission, are clearly evident in Tax-expressing cells.

Securin deficiencies in human and mouse cells have been shown to result in aberrant anaphase progression, chromosomal instability, and severe DNA aneuploidy (14, 19, 43). The data described here lend support to the importance of securin in safeguarding faithful chromosomal transmission during the cell cycle. Finally, the deficiencies in securin and cyclin B caused by Tax can explain why many adult T-cell leukemia cells are highly aneuploid (10) and large lymphocytes with cleaved/cerebriform nuclei, commonly known as flower or cloverleaf cells, appear at high frequency in blood smears from HTLV-1-seropositive individuals (23, 26, 38). These mitotic deficiencies are likely to play an important role in the leukemogenic process of HTLV-1.

The activity of Tax in promoting mitotic deficiencies immediately raises the question of how HTLV-1-transformed human T cells (MT2, MT4, and C8166) and Tax-transgenic mice manage to tolerate Tax expression at a high level without apparent abnormalities in cell division cycle or development. It is important to remember that transformed T cells, such as MT4, that express Tax constitutively have undergone tight selection during cell culture passage and should not be equated to the cells that expressed Tax for the first time after gene transduction, as described here. This interesting difference suggests that some cellular changes in MT4 and other HTLV-1-transformed T cells may have occurred to render Tax expression permissible. Mice that express the *tax* transgene under the transcriptional control of the HTLV-1 long terminal repeat fell into two classes, one with high levels of Tax expression in muscle, and another with high levels of Tax expression in thymus (30). The former mice developed soft tissue tumors, while the latter mice exhibited severe thymic atrophy and growth retardation and died soon after birth (29). It is conceivable that Tax expression in muscle did not cause mitotic defects because cells there are terminally differentiated and no longer cycling. It would be of interest to revisit the *tax*-transgenic mice that were growth retarded and with thymic atrophy to look for mitotic defects in their thymic tissue.

The cellular machineries that regulate cell cycle progression are highly conserved in evolution. For this reason, it is probably not surprising that the cell cycle effects of Tax can be recapitulated in *S. cerevisiae*. The result showing that the unscheduled reduction in Pds1p and Clb2p levels induced by Tax can be blocked by inactivation of APC or Cdc20p but not by inactivation of Cdh1p suggests that Tax promotes aberrant and premature activation of APC^{Cdc20p}. The activity of APC^{Cdc20p} is monitored by the spindle assembly checkpoint, which ensures proper attachment of the mitotic spindle to all chromosomes before APC^{Cdc20p} is activated for Pds1p destruction and sister chromatid separation (see references 2, 3, 5, and 11 for comprehensive reviews). In this manner, the spindle checkpoint safeguards the fidelity of chromosome transmission during mitosis. Late in mitosis, degradation of Cdc20p mediated by APC^{Cdh1} then allows APC to become associated with Cdh1 exclusively (33, 34). Cdh1 activity is further regulated by

Cdc14, a phosphatase sequestered in the nucleolus that becomes released and activated after anaphase and that catalyzes the removal of the inhibitory phosphate on Cdh1. Finally, phosphorylation of Cdh1 by cyclin A-Cdk2 and/or cyclin E-Cdk2 is thought to inactivate it during the interphase. Recent data from *Drosophila* and *Xenopus* cells indicate that a protein known as regulator of cyclin A (Rca1)/early mitotic inhibitor (Emi1), whose expression is driven by E2F during the G_1-S phase, can associate directly with APC^{Cdh1} and inhibit its activity before the onset of mitosis (12, 17, 42).

In Tax-expressing *S. cerevisiae* and HeLa cells, we detected an accumulation of Pds1p/securin and Clb2p/cyclin B late during the cell cycle progression, at 2 h (Fig. 3B) and 12 h (Fig. 6) after release from G_1/S arrest, respectively. Importantly, the level of each protein in these cells never reached the peak level achieved in Tax-null cells. Why have we never seen continued and constitutive degradation of Pds1p/securin and Clb2p/cyclin B at these "late" time points? We think this may be a consequence of APC^{Cdh1p}-mediated degradation of Cdc20p (33, 34). If the target of Tax is indeed APC^{Cdc20p}, as suggested by analysis of the *cdc20*^{ts} mutant (Fig. 4), then destruction of Cdc20p would effectively dampen the effect of Tax and allow some Pds1p/securin (and Clb2p/cyclin B) to accumulate. On the other hand, if the destruction of Cdc20p is prevented by deletion of the *CDH1* gene, then Tax should cause a severe degradation of Pds1p. Indeed, the Tax phenotype is much more pronounced in the *cdh1*-null background, in which the level of Pds1p in Tax-expressing *cdh1*-null cells is barely detectable (Fig. 4C), in sharp contrast to the Tax-negative *cdh1*-null and the Tax-expressing wild-type *CDH1* controls (Fig. 4C and Fig. 3C, respectively). Together, these results argue strongly that the target of Tax is APC^{Cdc20p}, not APC^{Cdh1p}.

Tax has been reported to cause a spindle checkpoint defect by interacting with the human spindle checkpoint protein MAD1 (21). More recently, it has been reported that in HTLV-1 Tax-expressing cells, human spindle assembly checkpoint factors HsMAD1 and HsMAD2 were mislocated from the nucleus to the cytoplasm (24). This altered localization of HsMAD1 and HsMAD2 apparently correlated with loss of mitotic checkpoint function. Although the interaction between Tax and HsMAD1 is particularly relevant in the context of this study, this interaction alone cannot explain the cell cycle aberrations described here, as Tax continued to cause growth arrest and cell cycle aberrations in a *mad-1*-null *S. cerevisiae* mutant (Fig. 4B). Furthermore, while Tax most likely acts via the spindle checkpoint, we do not think that Tax is inactivating the spindle checkpoint per se for the following reasons: first, Tax expression leads to multiple mitotic aberrations (outlined above) and a loss in cell viability; in contrast, cells without a functional spindle checkpoint (e.g., due to *MAD1* or *MAD2* deletion) are viable, albeit hypersensitive to spindle depolymerizing agents such as nocodazole; second, the absence of a functional spindle checkpoint does not lead to premature Pds1p/securin and Clb2p/cyclin B1 degradation and cell death, as seen in naïve cells made to express Tax.

Whether Tax usurps the spindle checkpoint apparatus to target the activation of APC^{Cdc20p} remains to be seen. In this vein, the wealth of information on cell cycle control in *S. cerevisiae* and the sophisticated genetics available for it are likely to facilitate a better understanding of the mechanism of action of Tax and the molecular basis for adult T-cell leukemia.

ACKNOWLEDGMENTS

We thank A. Amon, A. Murray, O. Cohen-Fix, and T. Dunn for yeast strains and plasmids; H. Zhou for human securin antibody; M. Yoshida and D. Morgan for recombinant adeno-Tax and adeno-tTA viruses; and X. Xiang and G. Han for assistance with microscopy.

This work was supported by grants RO1 CA48709 and RO1 CA/GM 75688 from the National Institutes of Health.

REFERENCES

1. **Akagi, T., H. Ono, and K. Shimotohno.** 1996. Expression of cell-cycle regulatory genes in HTLV-1 infected T-cell lines: possible involvement of Tax1 in the altered expression of cyclin D2, p18Ink4 and p21Waf1/Cip1/Sdi1. Oncogene **12:**1645–1652.
2. **Amon, A.** 1999. The spindle checkpoint. Curr. Opin. Genet. Dev. **9:**69–75.
3. **Amon, A.** 2001. Together until separin do us part. Nat. Cell Biol. **3:**12–14.
4. **Breeden, L. L.** 2000. Cyclin transcription: timing is everything. Curr. Biol. **10:**586–588.
5. **Burke, D. J.** 2000. Complexity in the spindle checkpoint. Curr. Opin. Genet. Dev. **10:**26–31.
6. **Chu, Z. L., Y. A. Shin, J. M. Yang, J. A. Di Donato, and L. H. Ballard, D. W.** 1999. IKKγ mediates the interaction of cellular IκB kinases with the tax transforming protein of human T-cell leukemia virus type 1. J. Biol. Chem. **274:**15297–15300.
7. **Cohen-Fix, O., and D. Koshland.** 1999. Pds1p of budding yeast has dual roles: inhibition of anaphase initiation and regulation of mitotic exit. Genes Dev. **13:**1950–1959.
8. **de la Fuente, C., F. Santiago, S. Y. Chong, L. Deng, T. Mayhood, P. Fu, D. Stein, T. Denny, F. Coffman, N. Azimi, R. Mahieux, and F. Kashanchi.** 2000. Overexpression of $p21^{waf1}$ in human T-cell lymphotropic virus type 1-infected cells and its association with cyclin A/cdk2. J. Virol. **74:**7270–7283.
9. **Fitch, I., C. Dahmann, U. Surana, A. Amon, K. Nasmyth, L. Goetsch, B. Byers, and B. Futcher.** 1992. Characterization of four B-type cyclin genes of the budding yeast *Saccharomyces cerevisiae*. Mol. Biol. Cell **3:**805–818.
10. **Fujimoto, T., T. Hata, T. Itoyama, H. Nakamura, K. Tsukasaki, Y. Yamada, S. Ikeda, N. Sadamori, and M. Tomonaga.** 1999. High rate of chromosomal abnormalities in HTLV-1-infected T-cell colonies derived from prodromal phase of adult T-cell leukemia: a study of IL-2-stimulated colony formation in methylcellulose. Cancer Genet. Cytogenet. **109:**1–13.
11. **Gardner, R. D., and D. J. Burke.** 2000. The spindle checkpoint: two transitions, two pathways. Trends Cell Biol. **10:**154–158.
12. **Grosskortenhaus, R., and F. Sprenger.** 2002. Rca1 inhibits APC-Cdh1(Fzr) and is required to prevent cyclin degradation in G_2. Dev. Cell **2:**29–40.
13. **Grossman, W. J., J. T. Kimata, F. H. Wong, M. Zutter, T. J. Ley, and L. Ratner.** 1995. Development of leukemia in mice transgenic for the *tax* gene of human T-cell leukemia virus type I. Proc. Natl. Acad. Sci. USA **92:**1057–1061.
14. **Hagting, A., N. Den Elzen, H. C. Vodermaier, I. C. Waizenegger, J. M. Peters, and J. Pines.** 2002. Human securin proteolysis is controlled by the spindle checkpoint and reveals when the APC/C switches from activation by Cdc20 to Cdh1. J. Cell Biol. **157:**1125–1137.
15. **Haller, K., T. Ruckes, I. Schmitt, D. Saul, E. Derow, and R. Grassmann.** 2000. Tax-dependent stimulation of G_1 phase-specific cyclin-dependent kinases and increased expression of signal transduction genes characterize HTLV type 1-transformed T cells. AIDS Res. Hum. Retroviruses **16:**1683–1688.
16. **Harhaj, E. W., and L. H. Sun, S. C.** 1999. IKKγ serves as a docking subunit of the IκB kinase (IKK) and mediates interaction of IKK with the human T-cell leukemia virus Tax protein. J. Biol. Chem. **274:**22911–22914.
17. **Hsu, J. Y., J. D. Reimann, C. S. Sorensen, J. Lukas, and P. K. Jackson.** 2002. E2F-dependent accumulation of hEmi1 regulates S phase entry by inhibiting APC(Cdh1). Nat. Cell Biol. **4:**433–442.
18. **Iha, H., T. Kasai, K. V. Kibler, Y. Iwanaga, K. Tsurugi, and K. T. Jeang.** 2000. Pleiotropic effects of HTLV type 1 Tax protein on cellular metabolism: mitotic checkpoint abrogation and NF-κB activation. AIDS Res. Hum. Retroviruses **16:**1633–1638.
19. **Jallepalli, P. V., I. C. Waizenegger, F. Bunz, S. Langer, M. R. Speicher, J. M. Peters, K. W. Kinzler, B. Vogelstein, and C. Lengauer.** 2001. Securin is required for chromosomal stability in human cells. Cell **105:**445–457.
20. **Jin, D. Y., V. Giordano, K. V. Kibler, H. Nakano, and L. H. Jeang.** 1999. Role of adapter function in oncoprotein-mediated activation of NF-κB. Human T-cell leukemia virus type I Tax interacts directly with IκB kinase γ. J. Biol. Chem. **274:**17402–17405.
21. **Jin, D. Y., F. Spencer, and K. T. Jeang.** 1998. Human T-cell leukemia virus

type 1 oncoprotein Tax targets the human mitotic checkpoint protein MAD1. Cell **93:**81–91.
22. **Kamihira, S.** 1992. Hemato-cytological aspects of adult T-cell leukemia. Gann Monogr. Cancer Res. **39:**17–32.
23. **Kasai, T., Y. Iwanaga, H. Iha, and K. T. Jeang.** 2002. Prevalent loss of mitotic spindle checkpoint in adult T-cell leukemia confers resistance to microtubule inhibitors. J. Biol. Chem. **277:**5187–5193.
24. **Lemasson, I., S. Thebault, C. Sardet, C. Devaux, and L. H. Mesnard, J. M.** 1998. Activation of E2F-mediated transcription by human T-cell leukemia virus type I Tax protein in a p16^{INK4A}-negative T-cell line. J. Biol. Chem. **273**:23598–23604.
25. **Liang, M. H., T. Geisbert, Y. Yao, S. H. Hinrichs, and C. Z. Giam.** 2002. Human T-lymphotropic virus type 1 oncoprotein tax promotes S-phase entry but blocks mitosis. J. Virol. **76:**4022–4033.
26. **Matutes, E., and D. Catovsky.** 1994. ATLL of Caribbean origin, p. 113–138. *In* Adult T-cell leukemia. Oxford University Press, Oxford, England.
27. **Minshull, J., A. Straight, A. D. Rudner, A. F. Dernburg, A. Belmont, and A. W. Murray.** 1996. Protein phosphatase 2A regulates MPF activity and sister chromatid cohesion in budding yeast. Curr. Biol. **6:**1609–1620.
28. **Nasmyth, K.** 2002. Segregating sister genomes: the molecular biology of chromosome separation. Science **297:**559–565.
29. **Nerenberg, M., S. H. Hinrichs, R. K. Reynolds, G. Khoury, and G. Jay.** 1987. The *tat* gene of human T-lymphotropic virus type 1 induces mesenchymal tumors in transgenic mice. Science **237:**1324–1329.
30. **Neuveut, C., and K. T. Jeang.** 2000. HTLV-1 Tax and cell cycle progression. Prog. Cell Cycle Res. **4:**157–162.
31. **Neuveut, C., K. G. Low, F. Maldarelli, I. Schmitt, F. Majone, R. Grassmann, and L. H. Jeang.** 1998. Human T-cell leukemia virus type 1 Tax and cell cycle progression: role of cyclin D-cdk and p110Rb. Mol. Cell. Biol. **18:**3620–3632.
32. **Ohtani, K., R. Iwanaga, M. Arai, Y. Huang, Y. Matsumura, and M. Nakamura.** 2000. Cell type-specific E2F activation and cell cycle progression induced by the oncogene product Tax of human T-cell leukemia virus type I. J. Biol. Chem. **275:**11154–11163.
33. **Peters, J. M.** 2002. The anaphase-promoting complex: proteolysis in mitosis and beyond. Mol. Cell **9:**931–943.
34. **Pfleger, C. M., and M. W. Kirschner.** 2000. The KEN box: an APC recognition signal distinct from the D box targeted by Cdh1. Genes Dev. **14:**655–665.
35. **Pfleger, C. M., E. Lee, and M. W. Kirschner.** 2001. Substrate recognition by the Cdc20 and Cdh1 components of the anaphase-promoting complex. Genes Dev. **15:**2396–2407.
36. **Pozzatti, R., J. Vogel, and G. Jay.** 1990. The human T-lymphotropic virus type I *tax* gene can cooperate with the *ras* oncogene to induce neoplastic transformation of cells. Mol. Cell. Biol. **10:**413–417.
37. **Sacher, R. A., N. L. Luban, D. I. Ameti, S. Friend, G. B. Schreiber, and E. L. Murphy.** 1999. Low prevalence of flower cells in USA blood donors infected with human T-lymphotropic virus types I and II. Br. J. Haematol. **105:**758–763.
38. **Schmitt, I., O. Rosin, P. Rohwer, M. Gossen, and R. Grassmann.** 1998. Stimulation of cyclin-dependent kinase activity and G_1- to S-phase transition in human lymphocytes by the human T-cell leukemia/lymphotropic virus type 1 Tax protein. J. Virol. **72:**633–640.
39. **Stemmann, O., H. Zou, S. A. Gerber, S. P. Gygi, and M. W. Kirschner.** 2001. Dual inhibition of sister chromatid separation at metaphase. Cell **107:**715–726.
40. **Surana, U., H. Robitsch, C. Price, T. Schuster, I. Fitch, A. B. Futcher, and K. Nasmyth.** 1991. The role of CDC28 and cyclins during mitosis in the budding yeast *S. cerevisiae*. Cell **65:**145–161.
41. **Tinker-Kulberg, R. L., and D. O. Morgan.** 1999. Pds1 and Esp1 control both anaphase and mitotic exit in normal cells and after DNA damage. Genes Dev. **13:**1936–1949.
42. **Vodermaier, H. C., and J. M. Peters.** 2002. Conspiracy to disarm APC in interphase. Nat. Cell Biol. **4:**119–120.
43. **Wang, Z., R. Yu, and S. Melmed.** 2001. Mice lacking pituitary tumor transforming gene show testicular and splenic hypoplasia, thymic hyperplasia, thrombocytopenia, aberrant cell cycle progression, and premature centromere division. Mol. Endocrinol. **15:**1870–1879.
44. **Weinstein, J.** 1997. Cell cycle-regulated expression, phosphorylation, and degradation of p55Cdc, a mammalian homolog of CDC20/Fizzy/slp1. J. Biol. Chem. **272:**28501–28511.
45. **Yamaoka, S., G. Courtois, C. Bessia, S. T. Whiteside, R. Weil, F. Agou, H. E. Kirk, R. J. Kay, and A. Israel.** 1998. Complementation cloning of NEMO, a component of the IκB kinase complex essential for NF-κB activation. Cell **93:**1231–1240.
46. **Yamaoka, S., H. Inoue, M. Sakurai, T. Sugiyama, M. Hazama, T. Yamada, and M. Hatanaka.** 1996. Constitutive activation of NF-κ B is essential for transformation of rat fibroblasts by the human T-cell leukemia virus type I Tax protein. EMBO J. **15:**873–887.
47. **Zachariae, W., and K. Nasmyth.** 1999. Whose end is destruction: cell division and the anaphase-promoting complex. Genes Dev. **13:**2039–2058.
48. **Zou, H., T. J. McGarry, T. Bernal, and M. W. Kirschner.** 1999. Identification of a vertebrate sister-chromatid separation inhibitor involved in transformation and tumorigenesis. Science **285:**418–422.